

Preparation of Photoactive Tungsten-doped Anatase Nanotubes Using Hydrothermal Technique

H.A. El Nazer and A.M. EL-Rafei^{*#}

Photochemistry Dept. and ^{}Refractories, Ceramics & Building Materials Dept., National Research Centre, Dokki, Cairo, Egypt. P.O. 12622.*

TITANIA (TiO₂) and tungsten doped titania (W-TiO₂) nanospheres were prepared by the sol-gel method, while tungsten doped titania nanotubes was formed by the hydrothermal process. The structure and the morphology of the prepared photocatalysts have been characterized using X-ray diffraction (XRD) and high resolution transmission electron microscope (HRTEM) techniques, respectively. XRD results of the W-TiO₂ powder, prepared by the sol - gel method and the hydrothermal method showed that anatase structure was formed. HRTEM images illustrate that the average diameter of the as-synthesized W-TiO₂ nanospheres was about 70 nm and the nanotubes ,W-TiO₂ NT, have an outer diameter ranging from 8 to 10 nm and inner diameter of 2 to 3 nm and a length of few hundreds of nanometers. The photocatalytic performance of the prepared photocatalysts was studied through the degradation of acid orange dye (AO7). Higher efficiency for degradation of AO7 was obtained using W-TiO₂ NT compared with TiO₂ and W-TiO₂ nano-powders. The results show that the dye removal was 99.88, 95.00 and 81.00 % within 60minutes in the case of using W-TiO₂ NT and W-TiO₂ nanospheres and TiO₂ nanospheres, respectively and the absorption edge shifts toward visible light region for both W- TiO₂ nano-powders and NT.

Keywords : Hydrothermal, Sol-gel, Nanotubes, Titanium dioxide, Tungsten doped titania.

Photocatalytic degradation of some organics has been studied using some metal oxide or sulfide photocatalysts. The most commonly studied photocatalysts include: TiO₂, ZnO, WO₃, Fe₂O₃, and ZnS⁽¹⁾.

The oxidation ability is an important factor for degradation of organics using photocatalytic oxidation technique. The photo generation of valence band holes (h_{vb}) and creation of hydroxyl radicals (HO• ads) are the key factors for using the photocatalyst in the degradation of organic compounds. This is also true if the excited conduction band electrons (e⁻_{cb}) have reducing power that is sufficient for the reduction of oxygen molecules to superoxide⁽²⁾.

The electron-hole pairs formation is considered to be an important key factor in the photocatalytic oxidation processes of organics for H₂O and CO₂. The energy of the semiconductor's band gap may define the irradiation energy that may be required

#Corresponding author emails: am.amin@nrc.sci.eg and amira_elrafei@yahoo.com

for excitation an electron from the valence band to the conduction band, resulting in leaving a positively charged hole in the valence band, h^+_{vb} . If the needed excitation energy of a given semiconductor to form charge carriers is outside the wavelength range of the incident irradiation energy, the photocatalyst is useless for the degradative oxidation of organic compounds without electronic modification⁽³⁻⁵⁾.

Titanium dioxide (TiO₂) photocatalyst has good oxidation ability as well as band gap energy that could absorb UV radiation. The ultraviolet radiation is considered to make up only about 5% of the solar energy. The doping of titanium dioxide with metals, non-metals and other metal oxides is of great interest for the improvement of visible light absorption and/or the decrement of recombination rate of excited electrons and holes. The reductive deposition of some noble metals (*e.g.* Pt or Au) onto the titanium dioxide surface is considered to be one of the most promising doping techniques. The splitting of water into H₂ and O₂ could not be carried out by photocatalysis techniques using undoped TiO₂. When nanoparticles of platinum are deposited on the surface of titanium dioxide, an increment in the H₂ production rate from adsorbed water molecules may be observed⁽⁶⁾. This may be attributed to the transfer of electrons from the TiO₂ surface to the metal resulting in the reduction of water molecules to hydrogen. The high prices of noble metals make them difficult to be used for industrial scale. Some transition metals, *i.e.* Fe and Cr, have been used as dopants; in conclusion, these metals are considered to act as electron and hole traps as well as decrease the recombination rate of electron hole pairs⁽⁷⁻¹⁰⁾.

Doping with tungstate has shown a shift of the band gap of TiO₂ to be closer to the visible spectrum (2.86 eV vs. 3.21 eV for pure anatase). This result is highly promising since increment the solar energy absorption is considered to be one of the important goals of titanium dioxide scientific research. The enhancement of photocatalytic degradation rate is also mentioned for many of these photocatalysts compared to pure anatase and Degussa. This improvement in the photocatalytic reaction may be attributed to an increment of surface acidity of the photocatalyst surface as well as the trapping of charge carriers^(11, 12). Azodyes are chemical dyes that are hazardous to environment⁽¹³⁾. The discharge of large amounts of these dyes into the environment via the dye effluents from textile mills causes problems for municipal wastewater treatment facilities.

The present work concerns with the preparation of TiO₂ nanosphere, W-TiO₂ nanosphere and W-TiO₂ nanotube photocatalysts. The oxidative efficiency of the prepared photocatalysts has been evaluated by the degradation of *azodye* such as Acid Orange 7 (AO7).

Experimental Procedures

Preparation of anatase & tungsten -doped anatase nanoparticles

A TiO₂ transparent sol was prepared by mixing of 17.5 g titanium(IV) butoxide Ti(O-nBu)₄ reagent grade (Sigma-Aldrich), 120 ml ethanol, 15 ml acetic acid, and 5 ml deionized water. The mixture was aged for 24 hr and was stirred at ambient
Egypt. J. Chem. **59**, No.6 (2016)

temperature. In case of preparation of tungsten doped titania, 60 ml of aqueous solution containing 4.56 g ammonium paratungstate (Sigma-Aldrich, $\geq 99\%$) $((\text{NH}_4)_{10}\text{W}_{12}\text{O}_{41}$, F.W.= 3042.55) was added under vigorous stirring to titania sol dropwise over 2 hr until the W-TiO₂ gel is formed. The TiO₂ gel was aged two days. The W-TiO₂ gel was then dried with a rotary evaporator at 150 °C. After drying, the samples were collected and ground using a mill. The TiO₂ powder was calcinated at 450 °C for three hours⁽¹⁴⁾.

Preparation of W-TiO₂ nanotubes

W-TiO₂ nanotubes were synthesized by the hydrothermal method. A conversion from nanoparticles to nanotubes was achieved by treating the W-TiO₂ nanoparticle with 10 M NaOH (ADWIC, 96%) at 150 °C for 24 hr in a Teflon-lined autoclave. The precipitates were neutralized thoroughly with HCl, then washed with deionized water, filtered and dried at 100°C. The detailed procedure is reported elsewhere^(15, 16).

Characterization

X-ray diffraction (XRD) analysis of the prepared powders was performed using BRUKER D8 ADVANCE with secondary monochromatic beam CuK α radiation at 40 Kv and 40 mA, whereas the microstructure of the prepared powders was examined using high resolution transmission electron microscope (HRTEM), JEOL, JEM-2100 working voltage at 200kV. The morphology of TiO₂ doped with tungsten was examined using Field emission scanning electron microscopy (FESEM) using JOEL Model JED-2300 instrument. The tungsten was observed by Energy-dispersive X-ray spectroscopy (EDX). The EDX spectra of the TiO₂ doped with tungsten was recorded on a JOEL Model JED-2300 instrument.

Photocatalytic experiments

The experiments were carried out using a photoreactor with fifteen fluorescent bulbs generating approximately 120 W m⁻² from 365-600 nm. Prior to irradiation, all of the samples were sonicated for 10 min to break up the photocatalyst agglomerates powder. During the photoreaction, the samples were stirred and the temperature held constant at 25-30 °C. For all runs, the amount of photocatalyst suspended in the dye solution was kept constant at 100 mg/l. the initial dye concentration was 250mg/l. The photocatalyst dose among the various runs was kept constant. A magnetic stirrer guaranteed satisfactory powder suspension and the uniformity of the reacting mixture. Oxygen was bubbled during this stage in order to ensure the availability of the oxidant gas in the solution. The irradiation time was taken at the moment when the lamp was switched on. Samples for analyses were withdrawn at fixed intervals of time. The dye concentration was analyzed using UV-visible spectrophotometer (Agilent-Carry 100). The maximum absorption wavelength for the acid orange 7 dye (λ_{max}) is 480 nm. The removal dye efficiency was estimated by applying the following Equation (1):

$$\text{Removal Dye Efficiency (\%)} = (C_0 - C / C_0) \times 100 \quad (1)$$

where C_0 is the original dye content and C is the residual dye in solution.

The chemical oxygen demand (COD) was determined by an open-reflux dichromate titrimetric procedure, as described in standard methods⁽¹⁷⁾.

Results and Discussions

Phase composition of the as-synthesized samples and hydrothermally treated samples

Figure 1 shows XRD patterns of the as-synthesized W-TiO₂ powder, prepared by the sol - gel method and hydrothermal method. As indicated in these patterns, both two samples exhibit anatase structure according to JCPDS 21-1272; *i.e.* 25.33(101), 37.88(004), 47.98(200), 54.74(105), 62.80(204), 70.00(116), 75.16 (301).

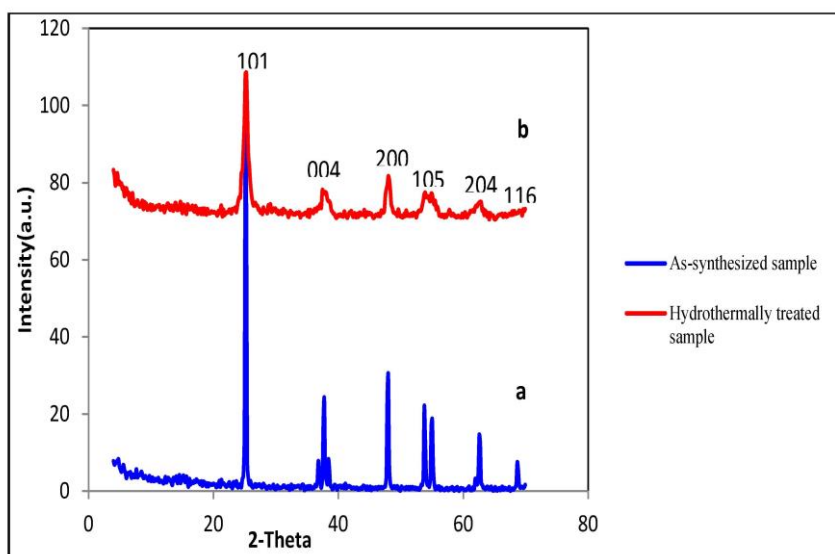
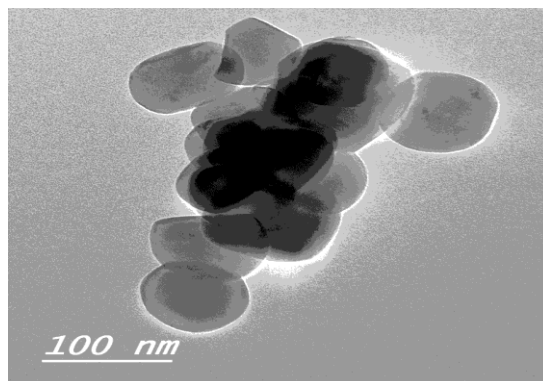


Fig. 1. XRD patterns of the as-synthesized W-doped TiO₂ powders: a) sol-gel sample b) Hydrothermally treated for 24 hr at 150 °C.

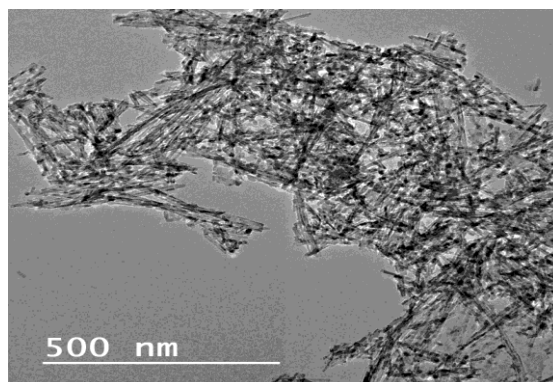
Morphology of as-synthesized W-TiO₂ and W- TiO₂ NT

Figure 2 (a, b and c) shows HRTEM images of as-synthesized W-TiO₂ nanoparticles and the obtained W-TiO₂ NT after the hydrothermal treatment with low and high-magnification, respectively. As-synthesized W-TiO₂ is nano-particle of pure anatase with an average diameter of about 70 nm as shown in Fig. 2(a).

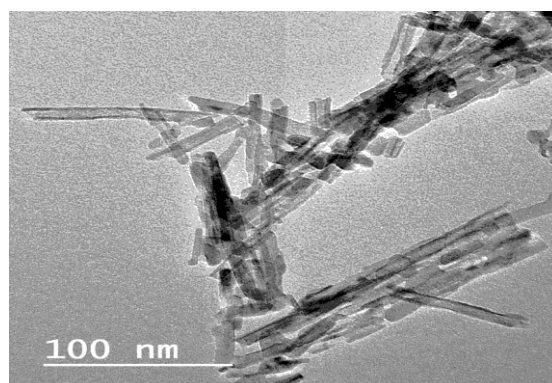
The as-grown W- TiO₂ NTs are generally homogeneous, (Fig.2b), fine hollow open-ended tubes with a uniform diameter along their lengths. The nanotubes have an outer diameter ranging from 8 to 10 nm and inner diameter of 2 to 3 nm and a length of few hundreds of nanometers, showing narrow size distribution, as shown in Fig.2(c). It is clear from these figures a well identified multi walled nanotubular structure can be formatted as it is clear from these figures.



(a)



(b)



(c)

Fig.2. Typical HR-TEM images of as-prepared a) W-doped TiO_2 and b) W-doped TNTs c) high-magnification W-doped TNTs.

One of the proposed mechanisms of the nanotube formation via the hydrothermal reaction is the formation of titanate containing alkali metal, first, during the hydrothermal treatment process using sodium hydroxide. Second, the ion exchange process of the alkali metal element has been occurred. The protonated titanate is then formed as a nano-sheet. Finally, the nano-sheet converts to be a tubular structure by scrolling process for lowering the surface energy⁽¹⁸⁾.

SEM/EDAX analysis of the W-TiO₂NTs

The SEM image revealed that the W-TiO₂ NT has smooth surfaces and uniformities in diameter size (Fig. 3a). Furthermore, the electron dispersive spectrum of the W-TiO₂ NT is made. From this EDX spectrum, (Fig. 3b), a very weak signal for W and a very strong signal for Ti can be observed. The quantitative analysis of the W-TiO₂ NT based on this spectrum showed that about 2.5 % of W was present. This is consistent with the nominal amount of doped tungsten.

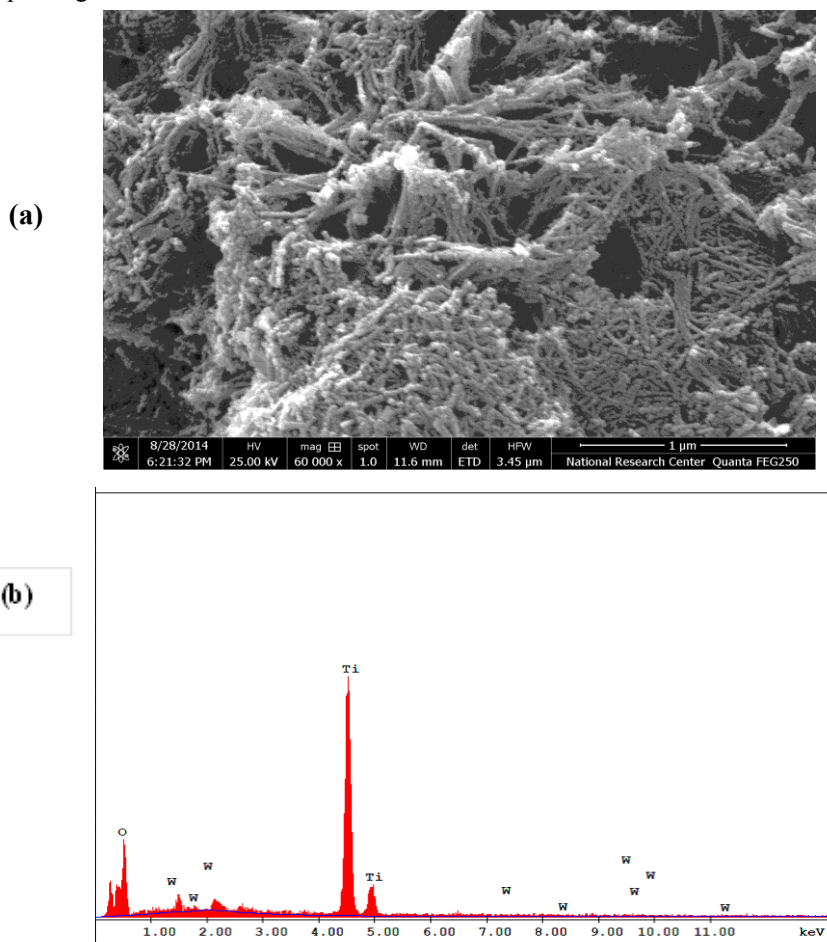


Fig. 3. (a) SEM image for W-doped W-TiO₂ NT, (b) EDS spectra for W-doped W-TiO₂ NT.

Photocatalytic performance

The photocatalytic degradation of AO7 was studied using the prepared photocatalysts. The structure of AO7 is shown in Fig. 4. The photolysis of AO7 dye was carried out in the absence of photocatalyst. The results showed that no significant dye or COD removal within 60 min of irradiation, (Fig. 5).

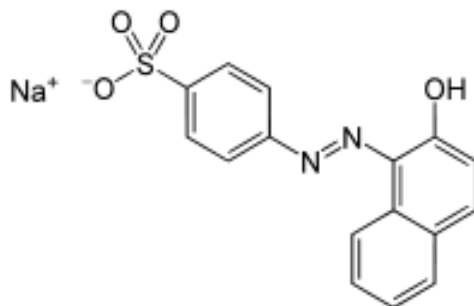


Fig. 4. Structure of Acid Orange (AO7) dye .

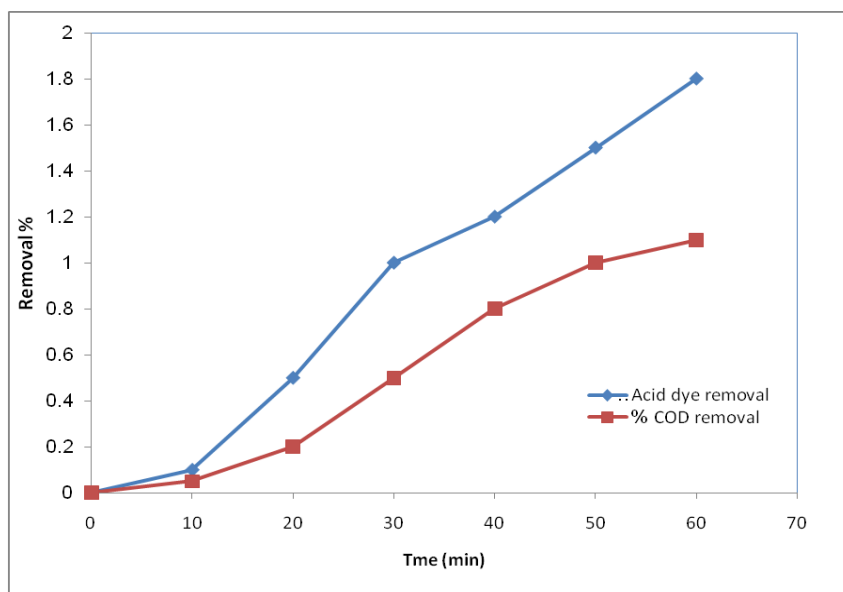


Fig. 5. Relationship between time of photolysis and the percentage of total dye and COD removal of acid orange dye in absence of Photocatalyst: pH= 5, and Temp= 25 °C.

The photocatalytic oxidation of AO7 experiment shows that the dye removal results were 99.88, 95.00 and 81.00 % in the case of using W-TiO₂ NT, W-TiO₂ nanospheres and TiO₂ nanospheres, respectively (Fig. 6). While the results of COD removal were

96.00, 90.00 and 62.00 % in the case of using W-TiO₂ NT, W-TiO₂ nanospheres and TiO₂ nanospheres, respectively, as shown in Fig. 7.

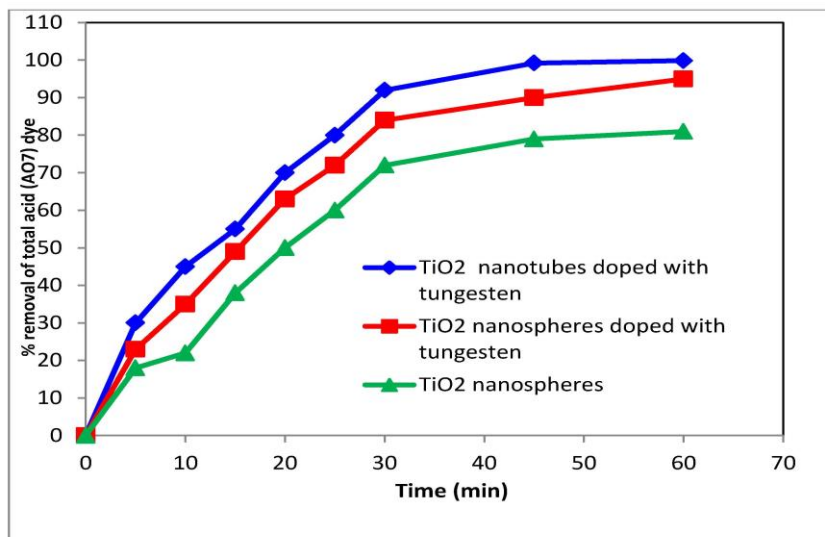


Fig. 6. Relationship between time of irradiation and the percentage of total Acid Orange dye removal using different photocatalysts. Photocatalyst: 100 mg l⁻¹, pH= 5 and Temp= 25 °C.

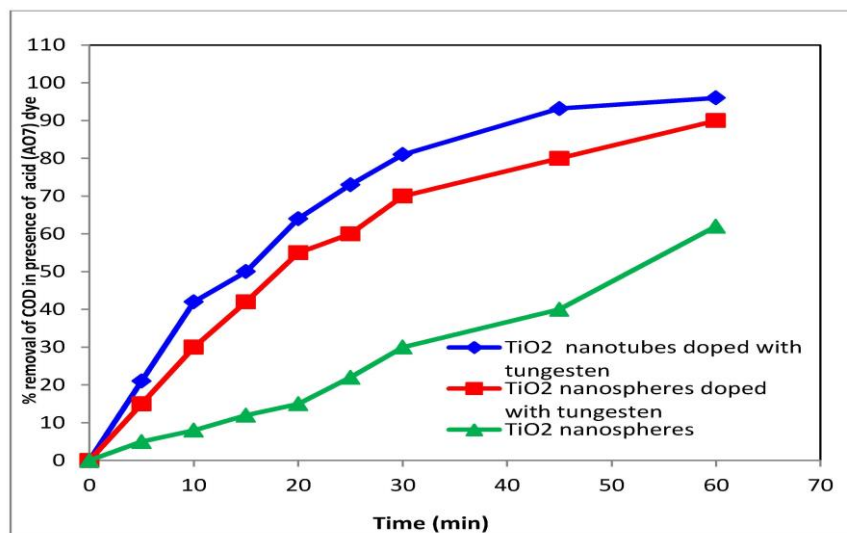


Fig. 7. Relationship between time of irradiation and the percentage of total COD removal in presence of acid orange dye using different photocatalysts. Photocatalyst: 100 mg l⁻¹, pH= 5, and Temp= 25 °C.

TiO₂ only exhibit the fundamental absorption band in the UV light region, while the absorption edge shifts towards the visible light region obviously for the W-TiO₂ and W-TiO₂ NT. The same behavior was observed with doping with earth ion⁽¹⁹⁾. The results indicate that the photocatalytic efficiency is relatively high in case of using nanotube morphology of TiO₂ due to increment in the photocatalyst surface area⁽²⁰⁾. This increment of photocatalytic efficiency was attributed to that when W ions in contact with the TiO₂ surface; it could trap excited electrons in the W-TiO₂ photocatalyst. During irradiation of W-TiO₂ photocatalyst, the excited electron may transfer from O²⁻ to W⁶⁺ and the W⁶⁺ reduces to W⁵⁺ as the electron trapping process is occurring. The oxidation of W⁵⁺ to W⁶⁺ may be performed by the oxygen present in the reaction mixture that could again trap the electrons resulting in increment of the photocatalytic activity⁽²¹⁾. Doping of TiO₂ with tungsten may form junction that contributes in the separation of the photogenerated electron-hole pairs. This may enhance the photocatalytic activity of the doped photocatalyst^(22,23). The crystallinity of nanotubes may decrease the electron-hole recombination probability in bulk as well as increase the diffusion efficiency of electrons and holes to adsorbed reactants on the TiO₂ surface to participate in the photocatalytic degradation reaction⁽²⁴⁾.

Conclusions

Titania (TiO₂) and tungsten doped titania (W-TiO₂) nanoparticles were prepared using sol-gel technique. Then transformation of tungsten doped titania nanoparticles into nanotubes (W-TiO₂ NT) was achieved using hydrothermal technique. Comparison of the photocatalytic activity of the three photocatalyst was made. The results of the photocatalytic oxidation of AO7 showed that the dye removal was 99.88, 95.00 and 81.00 % in the case of using W-TiO₂ NT, W-TiO₂ nanospheres and TiO₂ nanospheres, respectively and the absorption edge shifts towards visible light region obviously for the W-TiO₂ and W-TiO₂ NT. COD removal was 96.00, 90.00 and 62.00 % in the case of using W-TiO₂ NT, W-TiO₂ nanospheres and TiO₂ nanospheres, respectively.

References

1. **Fox, M.A.**, Heterogeneous photocatalysis, *Chem. Rev.* **93**, 341-357 (1993).
2. **Halmann, M.M.**, "Photodegradation of Water Pollutants"; CRC Press: New York (1996).
3. **Linsebigler, A.L., Lu, G. and Yates Jr., J.T.**, Photocatalysis on TiO₂ surfaces: principles, mechanisms, and selected results. *Chem. Rev.* **95**, 735-758 (1995).
4. **Jia, H. and He, W. et al.**, Generation of reactive oxygen species, electrons/holes, and photocatalytic degradation of rhodamine B by

- photoexcited CdS and Ag₂S micro-nano structures. *The Journal of Physical Chemistry, C* **118** (37), 21447-21456 (2014).
5. **Oppenländer, T.**, “*Photochemical Purification of Water and Air*”; Wiley-VCH: London (2003).
 6. **Emilio, C.A., Litter, M.I., Kunst, M., Bouchard, M. and Colbeau-Justin, C.**, [Phenol photodegradation on platinized-TiO₂ photocatalysts related to charge-carrier dynamics](#). *Langmuir*, **22**, 3606-3613 (2006).
 7. **Thompson, T.L. and Yates, J.T.**, Surface science studies of the photo activation of TiO₂-New photochemical processes. *Chem. Rev.* **106**, 4428-4453 (2006).
 8. **Isley, S.L. and Penn, R.L.**, Relative brookite and anatase content in sol-gel-synthesized titanium dioxide nanoparticles, *J. Phys. Chem. B* **110**, 15134-15139 (2006).
 9. **Zhang, Z. and Maggard, P.A.**, Investigation of photocatalytically-active hydrated forms of amorphous titania, TiO₂.nH₂O, *J. Photochem. Photobiol. A* **186**, 8-13 (2007).
 10. **Do, Y.R., Lee, W., Dwight, K. and Wold, A.**, The Effect of WO₃ on the photocatalytic activity of TiO₂. *J. Solid State Chem.* **108**, 198-201 (1994).
 11. **Wu, Q., Li, D., Chen, Z. and Fu, X.**, [New synthesis of a porous Si/TiO₂ photocatalyst: testing its efficiency and stability under visible light irradiation](#), *J. Photochem. Photobiol. Sci.* **5**, 653-655 (2006).
 12. **Engweiler, J., Harf, J. and Balkler, A.**, WO_x/TiO₂ catalysts prepared by grafting of tungsten alkoxides: morphological properties and catalytic behavior in the selective reduction of NO by NH₃. *J. Catal.* **159**, 259-269 (1995).
 13. **Jaimes-Ramírez, R., Vergara-Sánchez, J. and Silva-Martínez, S.**, Solar assisted degradation of acid orange 7 textile dye in aqueous solutions by Ce-doped TiO₂. *Mexican Journal of Scientific Research*, **1** (1), 42-55 (2012).
 14. **Li, X.Z., Li, F.B., Yang, C.L. and Ge, W.K.**, Photocatalytic activity of WO_x-TiO₂ under visible light irradiation. *J. Photochem. Photobiol. A* **141**, 209-217 (2001).
 15. **Kuen-Song Lin, Hao-Wei Cheng, Wen-Ru Chen and Chian-Fu Wu.** Synthesis, characterization, and adsorption kinetics of titania nanotubes for basic dye. *Wastewater Treatment Adsorption*, **16**, 47-56 (2010).

16. **Tomoko Kasuga**, Formation of titanium oxide nanotubes using chemical treatments and their characteristic properties. *Thin Solid Films*, **496**, 141 – 145 (2006).
17. **APHA, AWWA and WPCF**, “*Standard Methods for the Examination of Water and Wastewater*”, 20th ed., APHA, AWWA, WPCF, Washington, DC (1998).
18. **Tohru Sekino**, Synthesis and applications of titanium oxide nanotubes, “*Inorganic & Metallic Nanotubular materials, Recent Technologies and Applications*”, ISBN: 978-3-642-03620-0.
19. **Štengl, V., Bakardjieva, S. and Murafa, N.**, Preparation and photocatalytic activity of rare earth doped TiO₂ nanoparticles. *Materials Chemistry and Physics*, **114** (1), 217–226 (2009).
20. **Hahn, R., Schmidt-Stein, F., Salonen, J., Thiemann, S., Song, Y.Y., Kunze, J., Lehto, V.P. and Schmuki, P.**, Semimetallic TiO₂ nanotubes. *Angew. Chem.* **121**, 7372 (2009).
21. **Akurati, K.K., Vital, A., Dellemann, J.P., Michalow, K., Graule, T., Ferri, D. and Baiker, A.**, Flame-made WO₃/TiO₂ nanoparticles: relation between surface acidity, structure and photocatalytic activity. *Appl. Catal. B: Environ.* **79**, 53-62 (2008).
22. **Asiltürk, M., Sayilkan, F. and Arpac, E.**, Effect of Fe³⁺ ion doping to TiO₂ on the photocatalytic degradation of malachite green dye under UV and Vis-irradiation, *J. Photochem. Photobiol. A: Chem.* **203**, 64-71 (2009).
23. **Matos, J., Laine, J. and Herrmann, J.M.**, Synergy effect in the photocatalytic degradation of phenol on a suspended mixture of titania and activated Carbon. *Appl. Catal. B: Environ.* **18**, 281-291 (1998).
24. **JiaLin, Xiaolin Liu, Shu Zhu, Yongsheng Liu and Xianfeng Chen**, Anatase TiO₂ nanotube powder film with high crystallinity for enhanced photocatalytic performance. *Nanoscale Research Letters* **10**, 110 (2015).

(Received 31/10/2016;
accepted 25/12/2016)

تحضر ثاني أكسيد التيتانيوم (الأناتيز) المطعم بالتنجستن في صورة أنابيب نانومترية باستخدام المعالجة الحرارية المائية

حسام الدين عبد الفتاح الناظر و أميرة محمد الرافي*

قسم الكيمياء الضوئية و*قسم الحرارية والسيراميك ومواد البناء- المركز القومي للبحوث - الدقى - القاهرة- مصر - ص. ب. ١٢٦٢٢

تم في هذا البحث تحضير حوافر ضوئية كروية و أنبوبية في حجم النانو مصنوعة من ثاني أكسيد التيتانيوم (الأناتيز) و أيضا ثاني أكسيد التيتانيوم المطعم بعنصر التنجستن. واستخدمت تقنية المحلول الغروي في تحضير الحوافر الكروية و تقنية المعالجة الحرارية المائية في تحضير الحوافر الأنبوبية النانومترية، لتتم مقارنة النتائج المتحصل عليها باستخدام كلتا التقنيتين. و قد تم توصيف الحوافر المحضرة باستخدام تقنيات حيود الأشعة السينية و المجهر الإلكتروني النافذ ووضحت نتائج الأشعة السينية تكون طور الاناتيز. وأوضحت صور المجهر الإلكتروني النافذ أن متوسط قطر الكريات النانومترية لأكسيد التيتانيوم المطعم بالتنجستن كان حوالي ٧٠ نانومتر أما الأنابيب النانوية مترية فقد كان القطر الخارجي لها تتراوح من ٨ إلى ١٠ نانومتر، وقطرها الداخلي ٢-٣ نانومتر، و يبلغ طولها بضع مئات من النانومتر. وتم قياس كفاءة المحفزات الضوئية المحضرة في عملية الأكسدة الحفزية الضوئية للصبغة العضوية (البرتقالية الحامضية) في وجود الأشعة فوق بنفسجية و الضوء المرئي. وأوضحت النتائج العملية أن كفاءة الحافز الضوئي المحضر من ثاني أكسيد التيتانيوم المطعم بعنصر التنجستن في صورة الأنابيب النانومترية أعلى من المحضر في الصورة الكروية النانومترية حيث أن نسبة كفاءة تكسير الصبغة البرتقالية وصلت الى ٩٩,٨٨%. و أظهرت النتائج أيضا أن تطعيم الحافز الضوئي بعنصر التنجستن قد رفع من كفاءة امتصاص الحافز للضوء المرئي.